Neuroscience and Behavioral Physiology (2022) 52:769–777
https://doi.org/10.1007/s11055-022-01240-4

Influence of histone deacetylases inhibitor sodium butyrate on hippocampal neuronal activity *in vivo*

M. A. Roshchina[1] · A. A. Borodinova[1] · M. V. Roshchin[1]

Received: 26 March 2022 / Accepted: 20 April 2022

Abstract
Epigenetic regulation plays an important role in cognitive brain functions. The increase in histone acetylation by histone deacetylase inhibitors, such as sodium butyrate, was shown previously to be highly correlated with memory enhancement. Currently, the data on sodium butyrate effects on neuronal activity *in vivo* are limited. This study investigates how sodium butyrate affects the activity of CA1 hippocampal neurons in freely behaving mice. We performed *in vivo* calcium imaging of CA1 neurons with miniscopes in mice during arena exploration trials. The first trial was followed by an intraperitoneal injection of sodium butyrate or saline. After 45 and 90 minutes, CA1 neurons were recorded again in the homecage. The second trial was made 24 hours later. The injection of sodium butyrate resulted in immediate inhibition of neuronal activity for the following 90 minutes. However, the population activity analysis revealed that neurons that were active in the first behavioral trial demonstrated significantly more correlated activity during the second trial in the sodium butyrate group, but not in the saline group. Thus, for the first time, we demonstrated the effects of sodium butyrate on neuronal activity *in vivo*.

Keywords Epigenetics · Histone acetylation · Sodium butyrate · Calcium imaging · Hippocampus · Miniscopes

Introduction

Epigenetic modifications, such as histone acetylation, have been shown to play an important role in cognitive functions such as learning and memory through gene expression regulation [2]. Different physiological stimuli cause epigenetic modifications in the brain tissue, for example, the application of dopamine, acetylcholine, or glutamate receptor's agonists induced phosphorylation of Ser10 of H3 in different subfields of the hippocampus [6]. Induction of LTP in the prefrontal cortex was followed by a significant elevation of global H3 and H4 acetylation levels [34]. Learning and memory extinction in several cognitive tasks also changed histone acetylation level [10, 20].
Multiple studies have shown that sodium butyrate acts as a histone deacetylase (HDAC) inhibitor and thereby facilitates histone acetylation. Intraperitoneal injection of sodium butyrate led to significant growth of the amount of acetylated H3 and H4 histones in a brain within 30 minutes [8, 11, 30, 34, 35]. Repeated injections for 7 days increased the Arc,

✉ M. A. Roshchina
marina.zots@gmail.com

[1] Institute of Higher Nervous Activity and Neurophysiology of RAS, Moscow, Russia

Homer1, and Egr mRNA and protein levels in hippocampal neurons of the old mice [32]. Also, sodium butyrate injections increased the number of c-Fos-positive neurons in the infralimbic cortex after memory extinction in adult mice [33]. Sodium butyrate administration provided memory enhancement in multiple cognitive tasks, such as inhibitory avoidance, context fear conditioning, trace fear conditioning, Morris water maze, object location memory and novel object recognition tasks [3, 9, 16, 19, 26, 33–36].

There are a few studies on the effects of sodium butyrate on neuronal activity level, performed on acute brain slices. For example, the application of sodium butyrate enhanced the LTP induction in the hippocampus [20, 25] and the prefrontal cortex [34]. In contrast, a recent study [17] showed no significant effect on LTP after systemic sodium butyrate administration in wild-type mice. Interestingly, the same study reported LTP enhancement in 5xFAD mice. Regardless of the profuse data concerning sodium butyrate action on behavior, neuronal physiology *in vitro,* and molecular mechanisms, the effect of sodium butyrate on the neuronal activity in the brain of awake behaving animals remain poorly understood. To address this question, we recorded neuronal activity in the CA1 area of the dorsal hippocampus in freely behaving mice. To track the neuronal activity, we used calcium imaging of the GCamp6s-expressing neurons with a miniaturized head-mounted fluorescence microscope [1, 12]. Firstly, our experiments revealed a notable inhibition of neuronal activity during the first 45-90 minutes after sodium butyrate injection. Secondly, we analyzed the population properties of simultaneously recorded neurons and their correlations. Our data show that a subset of neurons that were active during two consecutive arena exploration sessions had more correlated activity in mice injected with sodium butyrate than in the saline-injected group. At the same time, the average neuronal activity correlation among all recorded neurons did not differ between conditions. Thus, we demonstrated for the first time the effects of HDAC inhibitor sodium butyrate administration on neuronal activity *in vivo* in the hippocampus of freely moving mice.

Methods

Animals

Experiments were conducted on adult male C57Bl/6 mice (breeding facility of the Institute of Bioorganic Chemistry RAS, Pushchino, Russia). Animals were kept in individual cages with *ad libitum* access to food and water on a 12-hour day-night cycle. Surgeries were performed on 3-months old mice and the experiments were carried oud approximately 3 months after. The study protocol (#012.09.2019) was approved by the Ethics Committee of the Institute of Higher Nervous Activity and Neurophysiology of RAS. All efforts were made to minimize the number of animals used and their potential suffering.

Drugs and injections

The histone deacetylase inhibitor sodium butyrate (NaB) (Sigma, USA) was freshly dissolved in sterile saline and injected intraperitoneally at a dose of 1.2 g/kg immediately after the first behavioral session (T1 session). Control mice were sham-injected with sterile saline. The injected liquid volume was 100 µl/10 g of animal weight.

Viral construct

Fluorescent protein calcium indicator GCamp6s [4] under control of the CAG promoter was packaged into recombinant adeno-associated virus serotype 2 (AAV2). Viral particles were produced according to standard protocols used for AAV preparation. Briefly, HEK293T cells were co-transfected with required plasmids using PEI reagent. On day 3 post-transfection, media and cells were collected and processed separately. Cells were harvested and subjected to three freeze/thaw cycles in liquid nitrogen. Supernatants were treated with polyethylene glycol (PEG8000),the PEG-precipitated AAVs were collected by centrifugation. AAV from cells and supernatant were mixed and treated with benzonase nuclease to destroy any unpacked DNA. Then the AAV particles were purified using a heparin column (HiTrap® Heparin columns). The required fraction, containing AAVs, was collected, filtered, and transferred to the Amicon Ultra-15 centrifugal filter unit for buffer exchange and concentration of virus suspension to the final volume of about 100 µl. Virus titer was then

determined by quantitative PCR using primer pair targeting AAV2 ITR sequence (Forward: GGAACCCCTAGTGATGGA GTT; Reverse: CGGCCTCAGTGAGCGA). To remove any extra-viral DNA before qPCR measurements, virus aliquots were treated with DNase I. Resulting virus titer was equal to 2.3E+13 μg/ml.
The AAV2 serotype is known to transduce mostly neuronal cells [29]. We have observed GCamp6s expression mostly in the pyramidal layer of CA1 of the hippocampus, but also in sparsely distributed cells located in other layers.

Stereotaxic surgeries

Three consecutive stereotaxic (Stoelting Co.) surgical manipulations were performed on mice keeping at least two-week intervals between them to recover. All procedures were made under isoflurane anesthesia (1.5% in oxygen 1 l/min) and local lidocaine analgesia. First, 1 μl of AAV2-pCAG-GCamp6s virus solution was slowly injected at a rate 0.1 μl/min into the dorsal CA1 area using a Gamilton syringe with a thin 30G steel needle attached. Injection coordinates were -2.3 mm from Bregma, 1.6 mm lateral, and -1.5 mm dorsoventral. Second, an opening in the skull was made, brain tissues below were partially removed and GRIN lens (1.8 mm diameter, Edmund Optics #64519) was gently placed above the CA1 hippocampal area and fixed to the skull using acrylic cement. The depth of the lens installation was adjusted stereotaxically so that only the pyramidal layer cells lay around the working distance of the GRIN lens. Third, the miniscope baseplate was attached in the position providing best focus on the neurons of interest.

Ca2+ imaging in freely behaving mice using a miniscope

Prior to experiments, each mouse was handled in the vivarium during one minute for three days. Next, for three more days we moved mice each day to the experimental room and installed a miniscope for 5-10 minutes. For three consecutive days mice were placed into the rectangular open-field arena (40 × 26 cm) with the miniscope attached (Fig. 1a). Mice were allowed to freely explore the arena for 3 minutes. On the fourth day, we placed two objects unfamiliar to mice in the arena (small dark bottles). Neuronal activity was recorded simultaneously with video recording of behavior during arena exploration (T1 session, 5 minutes long). Calcium imaging recordings were made at 30 frames per second (FPS) and at 752 × 480 px resolution with a miniscope (Miniscope, LabMaker UG, USA) (Fig. 1b). Mouse behavior was captured

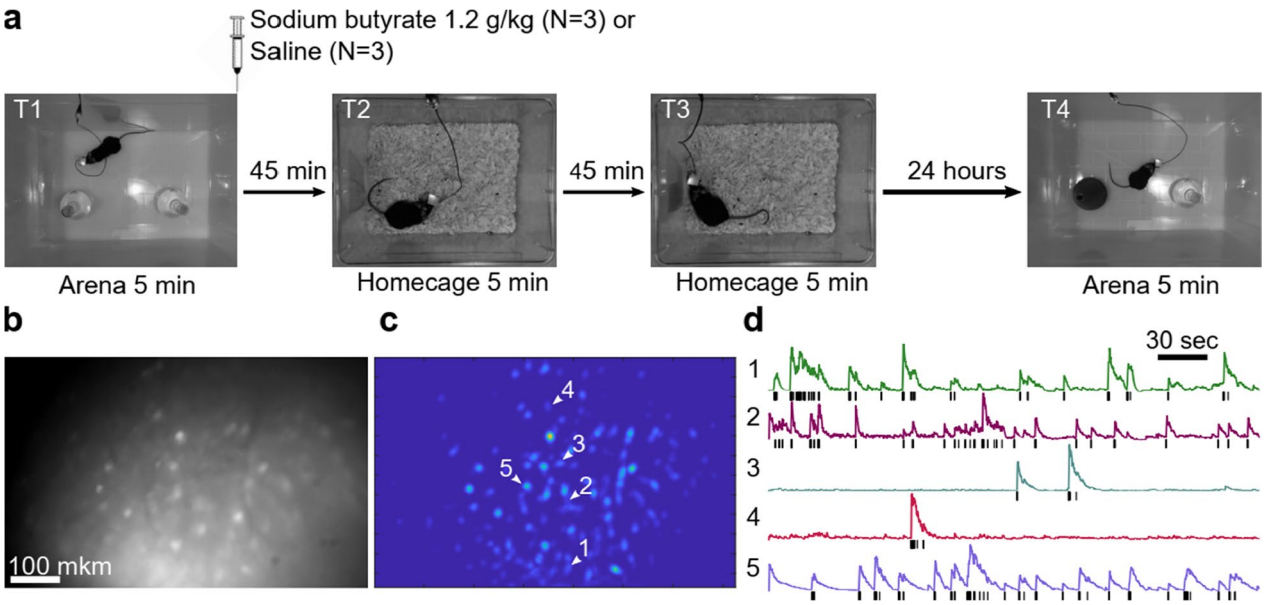

Fig. 1. Protocol and examples of recordings and processed results. **A**. Timeline of the experiment. **B**. Example raw recording of the GCamp6s-expressing neurons in CA1 area of the hippocampus. **C**. MIN1PIPE processing output: spatial footprints of active neurons. **D**. Example traces from several randomly selected neurons (marked with arrows in **C**). Black marks – spikes predicted by the CASCADE package

with a common USB web camera (Logitech) at 30 FPS. Immediately after the first trial mice were injected with NaB (n = 3) or saline (n = 3), and returned to their home cages. 45 and 90 min after injection we reattached the miniscope and performed two more imaging sessions (T2 and T3 sessions, 5 minutes long each) in their home cages. After the T3 session, mice were returned to the vivarium. Next day (~ 24h later) we replaced one of the old objects in the arena with a new one (a transparent round-bottom flask) and recorded one more session (5 minutes long). After the experiment, we performed a post-hoc morphological analysis of brain tissues to confirm the correct implantation of the GRIN lens.

Ca2+ imaging data processing

Prior to calcium signal analysis, the recorded images were manually aligned in FIJI [28] to remove large field of view shifts between sessions, and their spatial resolution was downsampled by factor of two. Calcium imaging videos were processed by the open-source pipeline MIN1PIPE [22], which includes modules for background removal, movement correction, automated ROI detection, and signal extraction based on the CNMF-e algorithm. A structural element for the initialization phase was set at 4 pixels. All extracted cell units were manually inspected. Each extracted unit was considered as an "active neuron" (Fig. 1c, d). In total, 1199 active neurons were detected in 6 mice.

Ca^{2+} signal from detected active neurons was deconvolved using the CASCADE package [27]. With this package, the dF/F traces extracted by MIN1PIPE were translated into expected spiking probabilities for each timepoint. The total number of spikes in each imaging session was calculated by summation of spike probability over time. Then the number of spikes in every session was divided by the duration of the session in seconds to calculate the spike rate.

Four imaging sessions were processed separately. Between sessions, matching of neurons was performed using the open-source probabilistic modeling package CellReg [31]. Co-registration was based on non-rigid alignment, maximal model distance set to 16 microns, probabilistic modeling based on spatial correlations, p-same threshold = 0.5.

For correlation and graph analysis, each neuron's activity was averaged over 1 s time bins. Pearson's correlation coefficient was computed for each pair of neurons in a given session. R-value was set to 0.3 according to the study by Jimenez et al. [18] in which the best noise reduction was achieved using that threshold [18]. The graph including all registered active neurons as nodes was constructed using the NetworkX python package [13]. Only the neurons with Pearson's correlation coefficient higher than the threshold value ($R > 0.3$) were connected by the graph edges. The correlated pair ratio (N of correlated pairs/ N of active neurons) was computed for each neuron and compared between sessions and mice.

Statistical analysis

Statistical analysis was performed using custom Python scripts based on data analysis packages NumPy, Matplotlib, and SciPy. The data are represented as mean ± standard deviation. In all cases, data were analyzed using a two-tailed t-test or a two-factor analysis of variance (ANOVA) with repeated measurements. Post-hoc analyses were conducted for the statistically significant main effects in ANOVA using Tukey's multiple comparisons test. All statistical tests used $p<0.05$ for the rejection of the null hypothesis.

Results

To investigate the effects of NaB on the *in vivo* neuronal activity, we recorded Ca^{2+} transients in the dorsal CA1 hippocampal neurons before injection (T1), 45 min later (T2), and 90 min later (T3) in the home cage, and, finally, 24 hours after the injection (T4).

We first analyzed the number of active neurons within the field of view during each trial. During T1 we detected 65 ± 34 active neurons in control mice and 62 ± 32 active neurons in a group "NaB" mice. Immediately after T1, the mice were injected with either saline (n = 3) or NaB (n = 3). Neuronal activity during subsequent trials demonstrated different dynamics in the two groups as shown in Fig. 2a. In the saline-injected mice the number of active neurons increased significantly both 45 min (113 ± 40 at T2) and 90 min (122 ± 25 at T3) after T1/injection, and then decreased almost to the T1 values 24 hours later (99 ± 47 at T4). In the NaB-injected group, we observed a short-lasting decrease in number of active neurons 45 min later (26 ± 14 at T2). 90 min later, the number of active neurons had almost restored (54 ± 24 at T3; 72 ± 20 at T4). Two-way repeated measures analysis of variance with factors "substance" (Saline or NaB) and "session"

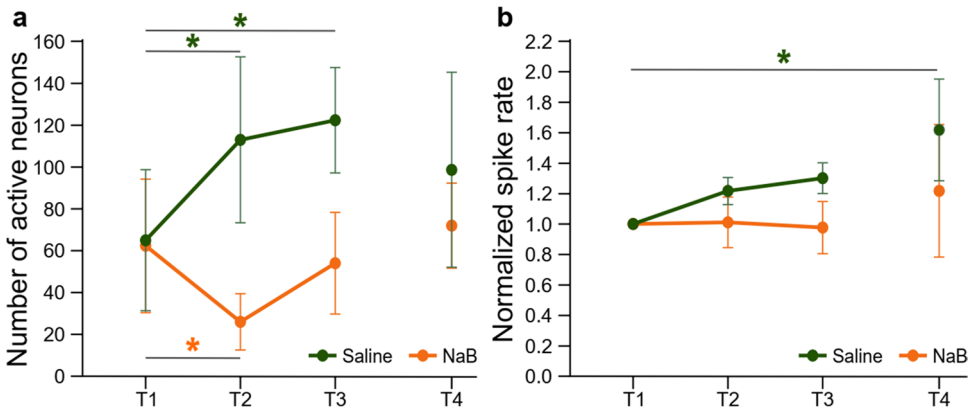

Fig. 2. Sodium butyrate (NaB) injection inhibited neuronal activity in the CA1 hippocampal area of freely behaving mice. **A**. Average number of active neurons in the field of view; the data indicate a decrease after injection of NaB but not after saline. **B**. Average spiking rate of all active neurons normalized to the first session; average spiking rate increased 24 hours after saline injection but did not change after injection of butyrate. * - $p < 0.05$, comparisons of T2, T3 or T4 timepoints with T1 (two-way repeated measures ANOVA followed by Tukey post-hoc analysis)

(T1, T2, T3, T4) revealed significant main effect of the "session" factor (F (3, 12) = 4.3, $p = 0.0281$) and a significant "substance × session" interaction (F (3, 12) = 11.14, $p = 0.0009$). Post-hoc analysis of the factor "session" indicated a significant increase of active neurons in T2 and T3 in comparison with T1 in saline-injected mice ($p = 0.006$ and $p = 0.002$, respectively, Tukey's multiple comparisons test). On the contrary, in NaB-injected mice, there was a significant decrease in T2 session relative to T1 ($p = 0.036$, Tukey's multiple comparisons test).

During the second stage of analysis, we investigated temporal properties of the active neurons. We predicted action potentials from calcium traces with the CASCADE package and calculated spiking rates for each neuron as the number of predicted spikes divided by session length in seconds. Average spiking rates in every trial were normalized by dividing by spiking rates during T1 (absolute values of spiking rate in T1 were 0.32 ± 0.06 spikes·s^{-1} before saline injection and 0.52 ± 0.06 spikes·s^{-1} before NaB injection). Average spiking rates slightly increased after the saline injection at all time points (1.22 ± 0.09 at T2, 1.3 ± 0.1 at T3, 1.62 ± 0.33 at T4) and did not change noticeably after the NaB injection (1.01 ± 0.17 at T2, 0.98 ± 0.17 at T3, 1.22 ± 0.44 at T4) (Fig. 2b). Two-way repeated measures ANOVA with factors of "substance" and "session" indicated a significant main effect of the "session" factor (F (3, 12) = 4.526, $p = 0.0242$) and "substance" factor (F (1, 4) = 10.25, $p = 0.0328$), but no factor interaction. Post-hoc analysis of factor "session" indicated a significant increase of the spiking rate in T4 in comparison with T1 in saline-injected mice ($p = 0.008$, Tukey's multiple comparisons test). Post-hos of the "substance" factor demonstrated no significant pairwise differences between two groups in all time points, including T4.

During the experiment, mice explored the experimental arena twice within a 24 hours interval (T1 and T4). We analyzed the number and spiking rates of neurons which were active during both trials in the arena with objects (T1&T4 neurons, they could be also active in homecage trials). The ratio of T1&T4 neurons to all the neurons active during T1 was slightly lower in NaB-injected mice than in control ones (41.6 ± 7.3 in saline mice, 28.3 ± 13.6 in NaB-injected mice, n.s. – $p > 0.05$, unpaired t-test) (Fig. 3a). The average spiking rate of the T1&T4 neurons insignificantly increased in the T4 session regardless of the injected substance (1.19 ± 0.32 s^{-1} at T4 after saline, 1.63 ± 0.57 s^{-1} at T4 after NaB; data normalized by T1 values, n.s. – $p > 0.05$ two-way ANOVA with repeated measures, Fig. 3b).

The miniscope recording technique allows to record activity of from tens to hundreds of neurons simultaneously and provides an opportunity to analyze the dynamics of neuronal networks *in vivo*. We identified the correlated pairs of neurons during each session T1-T4 and generated the network correlation graphs for each session. Next, we calculated the average correlated pairs ratio (Fig. 3c). Total correlated pairs ratio did not differ either in consecutive experimental trials or between NaB and control groups ($p > 0.05$, two-way ANOVA with repeated measures, Fig. 3d). However, if calculated solely for the neurons active during both T1&T4, the correlated pairs ratio demonstrated a significant increase at T4 in comparison to T1 after NaB but not saline injection (0.05 ± 0.14 at T1 and 0.25 ± 0.18 at T4 in NaB-injected mice, $p < 0.0001$, paired t-test, Fig. 3f; 0.14 ± 0.16 at T1 and 0.12 ± 0.15 at T4 in saline-injected mice, $p > 0.05$, paired t-test, Fig. 3e).

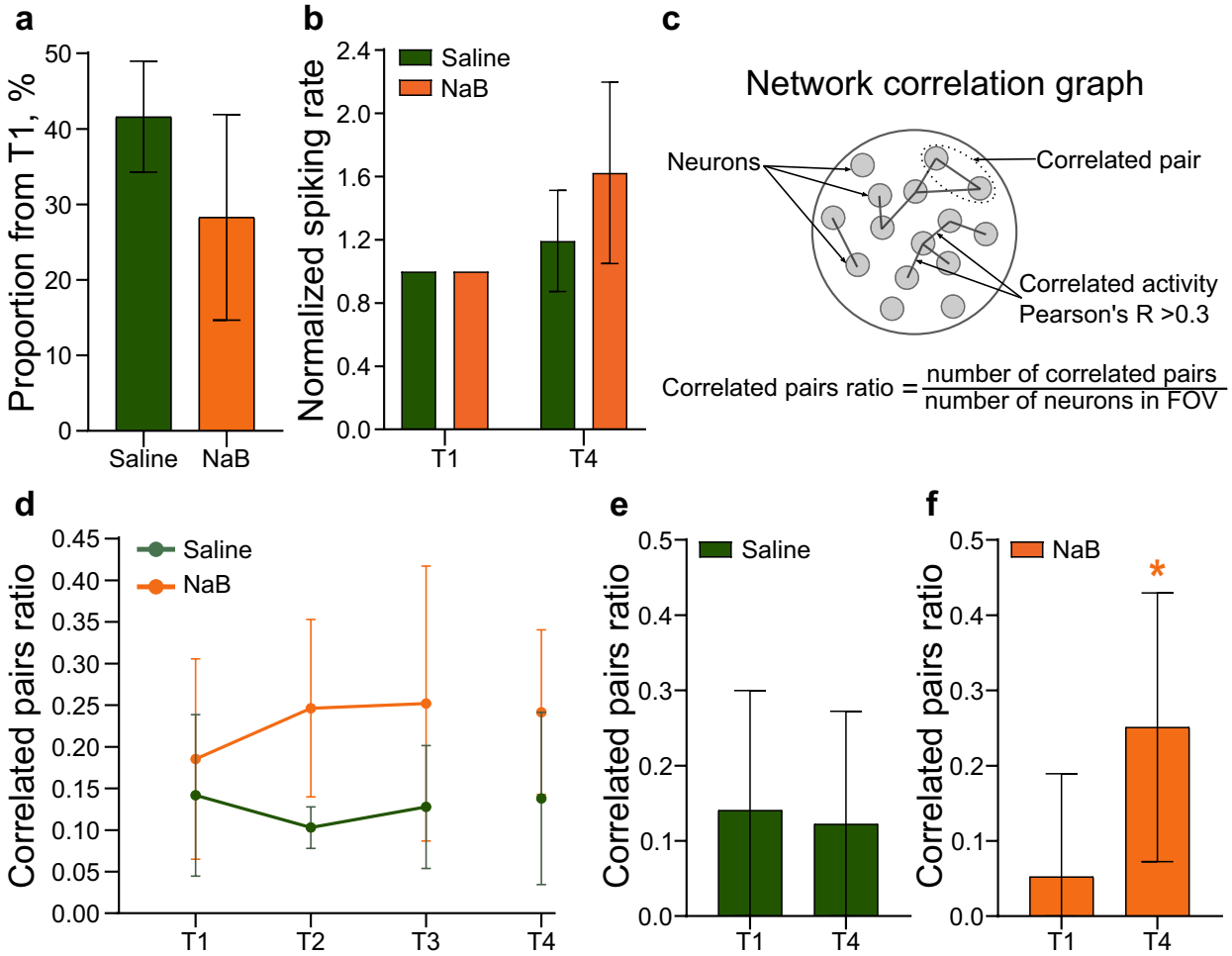

Fig. 3. Changes in network properties due to NaB administration. **A**. Average number of active neurons, reactivated from T1 to T4 showed a tendency to decrease after NaB but not saline (n.s.). **B**. Average spiking rate of reactivated T1&T4 neurons showed a tendency to increase from T1 session to T4 session in both groups (n.s.). **C**. Correlated graph analysis diagram. **D**. Average correlated pairs ratio did not differ between sessions or groups. **E**. Correlated pairs of reactivated T1&T4 neurons did not change after the saline injection. **F**. Correlated pairs ratio of reactivated T1&T4 neurons increased from T1 to T4 session after NaB injection. * - $p < 0.05$, comparison to T1 (paired two-tailed t-test)

Taken together, our results demonstrate two effects of NaB on neuronal activity in the CA1 hippocampal area *in vivo*. The short-term NaB action manifests in the decrease of the number of active neurons 45 min after the intraperitoneal administration. 24 hours after the injection, there were no differences in the number and spiking frequency of the neurons between NaB and saline mice. However, in the group of neurons activated during trials of arena exploration (T1&T4) the correlation pairs ratio increased after NaB but not saline injection.

Discussion

Previous studies have described the promnesic effects of sodium butyrate on different memory types in multiple behavioral paradigms [3, 9, 16, 19, 33, 34, 36]. Memory formation and storage processes depend on the neuronal activity both in the individual cells and interconnected populations. However, little was known yet about the effects of sodium butyrate on the physiological activity of the neurons *in vivo*. Few research papers made in acute brain slices described the LTP enhancement after sodium butyrate application [20, 34]. In order to expand the knowledge on the subject, we studied the effect of systemic administration of sodium butyrate on the activity of hippocampal neurons

in freely moving mice exploring the arena and then resting in home cages. One may assume that the new experience during arena exploration trial will induce neural plasticity. Based on the data obtained *in vitro,* sodium butyrate administration enhances the plasticity with the increased neural activity during the subsequent trial being a possible outcome. However, we observed a prominent decrease in neuronal activity. The effect peaked at 45 min and vanished 90 min after sodium butyrate administration. The timeline of the observed effect roughly fits the plasma concentration dynamics of the sodium butyrate described previously [7]. While there is a potential inconsistency between LTP experiments and our results, there is evidence of suppressive action of the sodium butyrate on neural activity [14, 15]. It must be emphasized that the studies were made in myenteric neurons in culture which might have very different properties than hippocampal neurons. It was shown in these studies that sodium butyrate causes the release of Ca^{2+} from the intracellular stores with the consequent activation of Ca^{2+}-dependent K^+ channels leading to hyperpolarization. One more possible explanation of the short-term effects of butyrate observed in our study is the indirect action of butyrate through stress-related mechanisms. Gagliano has shown that the glucose, adrenocorticotropic hormone and corticosterone levels in plasma increased 60 minutes after acute sodium butyrate injection at the dose of 1.2 g/kg (most commonly used dose) [11]. A higher dose of sodium butyrate (2.5 g/kg) also induced a body temperature drop and decreased GABA and glutamate concentrations in the brain [37]. Thus, the observed inhibition of the hippocampal neurons' activity in our study can be explained in two ways: the influence on electrical properties of neurons and an indirect impact via the stress-related regulation. However, the exact molecular mechanisms of sodium butyrate action were not the aim of our study and need further investigation. We should also mention the increase of average neuronal firing rate from T1 to T4 in saline group and similar but insignificant tendency in the sodium butyrate group. The increased neuronal activity may reflect either the memory about the experimental context by itself or some aversive memory trace produced by combination of the experimental context and following intraperitoneal injection.

Recently, much attention has been paid to the analysis of the population dynamics of neuronal ensembles during long-term memory maintenance. It has been shown that associative memory acquisition and storage are accompanied by increasing neuronal synchronization [21, 24]. So, we investigated the correlated activity of neurons reactivated during exploration of once visited familiar arena with objects. We found that the activity in this subset of neurons became significantly more correlated under the sodium butyrate action in comparison to the control group. The change in connectivity properties might be the potential mechanism of the promnesic effect of sodium butyrate.

One may cautiously speculate that both the effect of neuronal silencing (at average among the population) and the increase of synchronization of the cells being active during arena exploration later on are the reflections of the coexistence of homo- and heterosynaptic plasticity [5]. The process of the heterosynaptic LTD accompanying homosynaptic LTP was demonstrated a long time ago in the CA1 area [23]. Homosynaptic plasticity strengthens the synapses between active cells involved in the neural network underlying acquisition of the new experience during exploration and thus increases their connectivity, as revealed 24 hours later. At the same time, the heterosynaptic plasticity plays its role in suppressing the activity of the connections between not-involved neurons, leading to a decrease in overall activity.

Acknowledgments This study was supported by the grant of the Russian Science Foundation number 19-75-10067.
We thank Anna Gruzdeva and Walter Bast for editing the language of the manuscript.

Declarations

The authors declare that they have no competing financial or personal relationships that could have appeared to influence the work reported in this paper.

All data are available in the main text. Related data are available from the corresponding author on request.

REFERENCES

1. Aharoni D, Hoogland TM (2019) Circuit investigations with open-source miniaturized microscopes: Past, present and future. Front Cell Neurosci 13:1–12. https://doi.org/10.3389/fncel.2019.00141
2. Balaban PM, Borodinova AA (2019) Neurogenetic Technologies of Memory Maintenance Investigation. Russian Journal of Physiology. 105(11): 1392–1405. https://doi.org/10.1134/S0869813919110025
3. Blank M, Werenicz A, Velho LA, Pinto DF, Fedi AC, et al. (2015) Enhancement of memory consolidation by the histone deacetylase inhibitor sodium butyrate in aged rats. Neurosci Lett 594:76–81. https://doi.org/10.1016/j.neulet.2015.03.059

4. Chen TW, Wardill TJ, Sun Y, Pulver SR, Renninger SL, et al. (2013) Ultrasensitive fluorescent proteins for imaging neuronal activity. Nature 499(7458):295–300. https://doi.org/10.1038/nature12354
5. Chistiakova M, Bannon NM, Bazhenov M, Volgushev M. (2014) Heterosynaptic plasticity: Multiple mechanisms and multiple roles. Neuroscientist 20(5):483–98. https://doi.org/10.1177/1073858414529829
6. Crosio C, Heitz E, Allis CD, Borrelli E, Sassone-Corsi P (2003). Chromatin remodeling and neuronal response: Multiple signaling pathways induce specific histone H3 modifications and early gene expression in hippocampal neurons. J Cell Sci 116(24):4905–14. https://doi.org/10.1242/jcs.00804
7. Daniel P, Brazier M, Cerutti I, Pieri F, Tardivel I, et al. (1989) Pharmacokinetic study of butyric acid administered *in vivo* as sodium and arginine butyrate salts. Clin Chim Acta 181(3):255–63. https://doi.org/10.1016/0009-8981(89)90231-3
8. Dash PK, Orsi SA, Moore AN (2009) Histone deactylase inhibition combined with behavioral therapy enhances learning and memory following traumatic brain injury. Neuroscience 163(1):1–8. https://doi.org/10.1016/j.neuroscience.2009.06.028
9. Fischer A, Sananbenesi F, Wang X, Dobbin M, Tsai LH (2007) Recovery of learning and memory is associated with chromatin remodelling. Nature 447(7141):178–82. https://doi.org/10.1038/nature05772
10. Fontán-Lozano Á, Romero-Granados R, Troncoso J, Múnera A, Delgado-García JM, Carrión ÁM (2008) Histone deacetylase inhibitors improve learning consolidation in young and in KA-induced-neurodegeneration and SAMP-8-mutant mice. Mol Cell Neurosci 39(2):193–201. https://doi.org/10.1016/j.mcn.2008.06.009
11. Gagliano H, Delgado-Morales R, Sanz-Garcia A, Armario A (2014) High doses of the histone deacetylase inhibitor sodium butyrate trigger a stress-like response. Neuropharmacology 79:75–82. https://doi.org/10.1016/j.neuropharm.2013.10.031
12. Ghosh KK, Burns LD, Cocker ED, Nimmerjahn A, Ziv Y, et al. (2011) Miniaturized integration of a fluorescence microscope. Nat Methods 8(10):871–78. https://doi.org/10.1038/nmeth.1694
13. Hagberg A, Schult D, Swart P (2008) Exploring network structure, dynamics, and function using NetworkX. In: Varoquaux G, Vaught T, Millman J (Eds.) Proceedings of the 7th Python in Science conference (SciPy), pp. 11–15
14. Hamodeh SA, Rehn M, Haschke G, Diener M (2004) Mechanism of butyrate-induced hyperpolarization of cultured rat myenteric neurones. Neurogastroenterol Motil 16(5):597–604. https://doi.org/10.1111/j.1365-2982.2004.00545.x
15. Haschke G, Schäfer H, Diener M (2002) Effect of butyrate on membrane potential, ionic currents and intracellular ca2+ concentration in cultured rat myenteric neurones. Neurogastroenterol Motil 14(2):133–42. https://doi.org/10.1046/j.1365-2982.2002.00312.x
16. Intlekofer KA, Berchtold NC, Malvaez M, Carlos AJ, McQuown SC, et al. (2013) Exercise and sodium butyrate transform a subthreshold learning event into long-term memory via a brain-derived neurotrophic factor-dependent mechanism. Neuropsychopharmacology 38(10):2027–34. https://doi.org/10.1038/npp.2013.104
17. Jiang Y, Li K, Li X, Xu L, Yang Z (2021) Sodium butyrate ameliorates the impairment of synaptic plasticity by inhibiting the neuroinflammation in 5XFAD mice. Chem Biol Interact 341:109452. https://doi.org/10.1016/j.cbi.2021.109452
18. Jimenez JC, Berry JE, Lim SC, Ong SK, Kheirbek MA, Hen R (2020) Contextual fear memory retrieval by correlated ensembles of ventral CA1 neurons. Nat Commun 11(1):1–11. https://doi.org/10.1038/s41467-020-17270-w
19. Lattal KM, Barrett RM, Wood MA (2007) Systemic or Intrahippocampal Delivery of Histone Deacetylase Inhibitors Facilitates Fear Extinction. Behav Neurosci 121(5):1125–31. https://doi.org/10.1037/0735-7044.121.5.1125
20. Levenson JM, O'Riordan KJ, Brown KD, Trinh MA, Molfese DL, Sweatt JD (2004) Regulation of histone acetylation during memory formation in the hippocampus. J Biol Chem 279(39):40545–59. https://doi.org/10.1074/jbc.M402229200
21. Liu YZ, Wang Y, Shen W, Wang Z (2017) Enhancement of synchronized activity between hippocampal CA1 neurons during initial storage of associative fear memory. J Physiol 595(15):5327–40. https://doi.org/10.1113/JP274212
22. Lu J, Li C, Singh-Alvarado J, Zhou ZC, Fröhlich F, et al. (2018) MIN1PIPE: A Miniscope 1-Photon-Based Calcium Imaging Signal Extraction Pipeline. Cell Rep 23(12):3673–84. https://doi.org/10.1101/311548
23. Lynch GS, Dunwiddie T, Gribkoff V (1977) Heterosynaptic depression: a postsynaptic correlate of long-term potentiation. Nature 266:737–39. https://doi.org/10.1038/266737a0
24. Modi MN, Dhawale AK, Bhalla US (2014) CA1 cell activity sequences emerge after reorganization of network correlation structure during associative learning. Elife 2014(3):1–25. https://doi.org/10.7554/eLife.01982
25. Pandey K, Sharma KP, Sharma SK (2015) Histone deacetylase inhibition facilitates massed pattern-induced synaptic plasticity and memory. Learn Mem 22(10):514–18. https://doi.org/10.1101/lm.039289.115
26. Roozendaal B, Hernandez A, Cabrera SM, Hagewoud R, Malvaez M, et al. (2010) Membrane-associated glucocorticoid activity is necessary for modulation of long-term memory via chromatin modification. J. Neurosci 30(14):5037–46. https://doi.org/10.1523/JNEUROSCI.5717-09.2010
27. Rupprecht P, Carta S, Hoffmann A, Echizen M, Blot A, et al. (2021) A database and deep learning toolbox for noise-optimized, generalized spike inference from calcium imaging. Nat Neurosci 24(9):1324–37. https://doi.org/10.1038/s41593-021-00895-5
28. Schindelin J, Arganda-Carreras I, Frise E, Kaynig V, Longair M, et al. (2012) Fiji: An open-source platform for biological-image analysis. Nat Methods 9(7):676–82. https://doi.org/10.1038/nmeth.2019
29. Schober AL, Gagarkin DA, Chen Y, Gao G, Jacobson L, Mongin AA (2016) Recombinant Adeno-Associated Virus Serotype 6 (rAAV6) Potently and Preferentially Transduces Rat Astrocytes In vitro and In vivo. Front Cell Neurosci 10:262. https://doi.org/10.3389/fncel.2016.00262
30. Schroeder FA, Lin CL, Crusio WE, Akbarian S (2007) Antidepressant-Like Effects of the Histone Deacetylase Inhibitor, Sodium Butyrate, in the Mouse. Biol Psychiatry 62(1):55–64. https://doi.org/10.1016/j.biopsych.2006.06.036
31. Sheintuch L, Rubin A, Brande-Eilat N, Geva N, Sadeh N, et al. (2017) Tracking the Same Neurons across Multiple Days in Ca2+ Imaging Data. Cell Rep 21(4):1102–15. https://doi.org/10.1016/j.celrep.2017.10.013
32. Singh P, Thakur MK (2018) Histone Deacetylase 2 Inhibition Attenuates Downregulation of Hippocampal Plasticity Gene Expression during Aging. Mol Neurobiol 55(3):2432–42. https://doi.org/10.1007/s12035-017-0490-x

33. Stafford JM, Raybuck JD, Ryabinin AE, Lattal KM (2012) Increasing histone acetylation in the hippocampus-infralimbic network enhances fear extinction. Biol Psychiatry 72(1):25–33. https://doi.org/10.1016/j.biopsych.2011.12.012
34. Sui L, Wang Y, Ju LH, Chen M (2012) Epigenetic regulation of reelin and brain-derived neurotrophic factor genes in long-term potentiation in rat medial prefrontal cortex. Neurobiol Learn Mem 97(4):425–40. https://doi.org/10.1016/j.nlm.2012.03.007
35. Villain H, Florian C, Roullet P (2016) HDAC inhibition promotes both initial consolidation and reconsolidation of spatial memory in mice. Sci Rep 6(May):1–9. https://doi.org/10.1038/srep27015
36. Vinarskaya AK, Balaban PM, Roshchin M V., Zuzina AB (2021) Sodium butyrate as a selective cognitive enhancer for weak or impaired memory. Neurobiol Learn Mem 180:107414. https://doi.org/10.1016/j.nlm.2021.107414
37. Xu Y, Peng S, Cao X, Qian S, Shen S, et al. (2021) High doses of butyrate induce a reversible body temperature drop through transient proton leak in mitochondria of brain neurons. Life Sci 278:119614. https://doi.org/10.1016/j.lfs.2021.119614